GEOPHYSICS, VOL. 87, NO. 1 (JANUARY-FEBRUARY 2022); P. M13–M24, 14 FIGS.
10.1190/GEO2021-0177.1

Markov chain Monte Carlo for petrophysical inversion

Dario Grana[1], Leandro de Figueiredo[2], and Klaus Mosegaard[3]

ABSTRACT

Stochastic petrophysical inversion is a method used to predict reservoir properties from seismic data. Recent advances in stochastic optimization allow generating multiple realizations of rock and fluid properties conditioned on seismic data. To match the measured data and represent the uncertainty of the model variables, many realizations are generally required. Stochastic sampling and optimization of spatially correlated models are computationally demanding. Monte Carlo methods allow quantifying the uncertainty of the model variables but are impractical for high-dimensional models with spatially correlated variables. We have developed a Bayesian approach based on an efficient implementation of the Markov chain Monte Carlo (MCMC) method for the inversion of seismic data for the prediction of reservoir properties. Our Bayesian approach includes an explicit vertical correlation model in the proposal distribution. It is applied trace by trace, and the lateral continuity model is imposed by using the previously simulated values at the adjacent traces as conditioning data for simulating the initial model at the current trace. The methodology is first presented for a 1D problem to test the vertical correlation, and it is extended to 2D problems by including the lateral correlation and comparing two novel implementations based on sequential sampling. Our method is applied to synthetic data to estimate the posterior distribution of the petrophysical properties conditioned on the measured seismic data. The results are compared with an MCMC implementation without lateral correlation and demonstrate the advantage of integrating a spatial correlation model.

INTRODUCTION

One of the main goals of reservoir characterization is to build models of petrophysical properties, including porosity, mineralogy, and fluid saturations. The available data include direct measurements of the petrophysical properties of interest at sparse well locations, namely, well logs, and indirect measurements of their geophysical response measured at the surface, namely, seismic surveys. Petrophysical properties can be predicted from well log and seismic data by combining inverse theory with geophysical equations such as seismic and rock-physics modeling (Aki and Richards, 1980; Avseth et al., 2010; Mavko et al., 2020). If the petrophysical properties are known, then the seismic response can be computed using rock physics and seismic models. Because the petrophysical properties are unknown and the seismic response is measured, the modeling problem is formulated as an inverse problem. Deterministic methods such as gradient-based approaches can be applied to predict the petrophysical properties. However, the solution, i.e., the model of petrophysical properties, is not unique due to the presence of noise in the data, limited resolution of the seismic data, and the approximations of the physical operators linking the model to the measured data. Probabilistic methods are then preferable because they provide a prediction of the most likely model and its uncertainty. The solution of the probabilistic inverse problem can be expressed using probability distributions or multiple model realizations. Doyen (2007), Bosch et al. (2010), Azevedo and Soares (2017), and Grana et al. (2021) provide a review of the main seismic reservoir characterization methods developed for hydrocarbon reservoirs.

Bayesian inversion methods for seismic and petrophysical inversion have been proposed in geophysics literature (Tarantola and Valette, 1982; Sen and Stoffa, 1996; Scales and Tenorio, 2001; Ulrych et al., 2001; Buland and Omre, 2003; Tarantola, 2005). For example, Buland and Omre (2003) derive an efficient solution for seismic inversion for the prediction of elastic properties (i.e., velocities or

Manuscript received by the Editor 15 March 2021; revised manuscript received 31 August 2021; published online 12 November 2021.
[1]University of Wyoming, Laramie, Wyoming 82071, USA. E-mail: dgrana@uwyo.edu (corresponding author).
[2]LTrace, Santa Catarina 88032, Brazil. E-mail: leandrop.fgr@gmail.com.
[3]University of Copenhagen, Copenhagen 2100, Denmark. E-mail: mosegaard@nbi.ku.dk.

impedances), but their approach requires the linearization of the forward operator. Their approach has been extended to petrophysical inversion and lithofluid classification (Larsen et al., 2006; Buland et al., 2008; Grana and Della Rossa, 2010; Ulvmoen and Omre, 2010; Rimstad et al., 2012; Grana, 2016; Jullum and Kolbjørnsen, 2016; Grana et al., 2017). However, rock-physics models are generally nonlinear, and their linearization might lead to inaccurate predictions, for example, for fluid saturations. Furthermore, sampling the posterior distribution of the petrophysical variables presents several challenges because petrophysical properties are bounded between zero and one, multimodal, and spatially correlated due to geologic continuity. Pioneering works on the use of geostatistical sampling methods include Doyen (1988), Bortoli et al. (1993), and Haas and Dubrule (1994). Geostatistical inversion methods based on stochastic sampling have been later developed in several publications (Soares et al., 2007; González et al., 2008; Grana et al., 2012; Jeong et al., 2017; Azevedo et al., 2015, 2020; de Figueiredo et al., 2019a, 2019b; Cyz and Azevedo, 2020).

The application of stochastic inversion methods to geophysical problems for the prediction of petrophysical variables is challenging due to non-Gaussian distributions, spatial correlation, and data conditioning. Markov chain Monte Carlo (MCMC) are statistical algorithms to sample the probability distribution of a random variable and can be applied to geophysical inverse problems to sample the posterior distribution of the model variables conditioned on the measured data (Mosegaard and Tarantola, 1995; Sambridge and Mosegaard, 2002). Mukerji et al. (2001) and Eidsvik et al. (2004) adopt an MCMC approach to compute the posterior model of the reservoir variables conditioned on the available observations and predict the lithofluid facies in the reservoir. The approach is applied using a categorical variable with a finite number of facies values. Hansen et al. (2012) and Zunino et al (2015) present MCMC methods that efficiently incorporate complex prior models into the inverse problem. Connolly and Hughes (2016) present a Monte Carlo approach in which realizations are sampled from a prior distribution and accepted or rejected based on the data mismatch. The method includes a vertical correlation model and a Markov chain for the categorical variable, but it does not include a lateral continuity model. De Figueiredo et al. (2019a, 2019b) present an MCMC method that can be applied to discrete and continuous variables and include a spatial correlation model, but the convergence for nonlinear models is much slower than for the linear case. Similarly, Aleardi and Salusti (2020a, 2020b) present different formulations of the MCMC approach using different prior distributions and probability ratios. Non-Bayesian seismic and petrophysical inversion methods have also been applied, using nonlinear regressions, gradient-based optimization, or deep-learning algorithms (Priezzhev et al., 2019; Babasafari et al., 2021).

We propose an MCMC method for the joint prediction of petrophysical properties, for example, porosity and water saturation, conditioned on partially stacked seismic data. The methodology is based on a 1D implementation, in which the petrophysical properties are iteratively simulated from multivariate distributions with a vertical correlation model to match the measured data. We then propose an efficient implementation of the MCMC method for 2D applications by adopting a sequential approach based on the 1D sampling MCMC approach with a local preconditioning prior model depending on the previously inverted traces. We introduce two different implementations in which the local preconditioning prior model is based on kriging and sequential sampling, respectively, to impose the lateral correlation model in the solution. The method is demonstrated in 1D and 2D petrophysical inversion problems and estimates the posterior distribution of the petrophysical variables conditioned on the seismic data.

METHODOLOGY

We formulate the inverse problem in a general way such that it can be applied to any set of model variables and any geophysical data for which the forward problem is known. Given a set of measurements $\mathbf{d}$, we aim to predict the model variables $\mathbf{m}$ that generated the measurements based on the geophysical function $\mathbf{f}:\mathbb{R}^{n_m} \rightarrow \mathbb{R}^{n_d}$ that approximates the physical processes as

$$\mathbf{d} = \mathbf{f}(\mathbf{m}) + \boldsymbol{\varepsilon}, \tag{1}$$

where $\boldsymbol{\varepsilon}$ represents the error in the data. In this formulation, we assume that the error due to the approximations of the physical models is negligible compared to the data error; however, the approach could be extended to modeling errors as shown in Hansen et al. (2014). The geophysical operator $\mathbf{f}$ is assumed to be nonlinear. We focus on petrophysical inversion problems, where $\mathbf{m}$ represents the porosity and water saturation, $\mathbf{d}$ represents the partially stacked seismic data, and $\mathbf{f}$ is a function that combines the seismic amplitude-variation-with-offset model with a rock-physics model. We also assume that model variables and data are represented by vectors of finite length; therefore, $\mathbf{m}$ is a vector of length n_m and $\mathbf{d}$ and $\boldsymbol{\varepsilon}$ are vectors of length n_d. For 1D univariate applications, n_d is the number of samples of the seismic trace, and $n_m = n_d + 1$, whereas for multivariate applications, n_d depends on the number of samples and the number of angle stacks, and n_m depends on the number of samples and the number of variables. For 2D and 3D applications, n_d and n_m also depend on the number of seismic traces. The errors are assumed to be independent and Gaussian distributed with mean $\mathbf{0}$ and covariance matrix $\boldsymbol{\Sigma}_\varepsilon$. If the seismic errors are assumed to be spatially uncorrelated, the covariance matrix $\boldsymbol{\Sigma}_\varepsilon$ is then diagonal, whereas, in the general case, $\boldsymbol{\Sigma}_\varepsilon$ is a full matrix that depends on the spatial correlation model of the error.

The probabilistic solution of the inverse problem is the posterior probability density function (PDF) commonly called the posterior distribution $P(\mathbf{m}|\mathbf{d})$ that, according to Bayes' rule, is proportional to the likelihood function $P(\mathbf{d}|\mathbf{m})$ and the prior PDF or prior distribution $P(\mathbf{m})$:

$$P(\mathbf{m}|\mathbf{d}) = \frac{P(\mathbf{d}|\mathbf{m})P(\mathbf{m})}{P(\mathbf{d})}, \tag{2}$$

where $P(\mathbf{d})$ is a constant. In the linear-Gaussian case (univariate or multivariate), the solution of the inverse problem can be estimated analytically (Buland and Omre, 2003; Tarantola, 2005; Hansen et al., 2006), whereas in the nonlinear case the solution must be assessed numerically.

We assume that the prior PDF of the model variable $\mathbf{m}$ (i.e., the vector of the model variables at the spatial locations of interest) is Gaussian $\mathcal{N}(\mathbf{m};\boldsymbol{\mu}_m,\boldsymbol{\Sigma}_m)$ with locally variable prior mean $\boldsymbol{\mu}_m$ and spatially correlated prior covariance matrix $\boldsymbol{\Sigma}_m$. The prior mean $\boldsymbol{\mu}_m$ is assumed to be given by a low-frequency background trend based on prior geologic information, whereas the prior covariance matrix $\boldsymbol{\Sigma}_m$ is obtained by combining the stationary (spatially independent) covariance matrix $\boldsymbol{\Sigma}_m^0$ of the model variables and the vertical

correlation matrix $\mathbf{\Sigma}_t$ associated with correlation function $v(t)$, for example, using the Kronecker product $\mathbf{\Sigma}_m^0 = \mathbf{\Sigma}_m^0 \otimes \mathbf{\Sigma}_t$. The likelihood function of $\mathbf{d}|\mathbf{m}$ is assumed to be Gaussian $\mathcal{N}(\mathbf{d}; \mathbf{f}(\mathbf{m}), \mathbf{\Sigma}_\varepsilon)$ with mean $\mathbf{f}(\mathbf{m})$ and spatially independent covariance matrix $\mathbf{\Sigma}_\varepsilon$. Because the forward operator $\mathbf{f}$ is not linear, the resulting posterior distribution of $\mathbf{m}|\mathbf{d}$ is not Gaussian and must be assessed numerically.

MCMC algorithms are iterative methods in which the solution is updated at each iteration. After an initial burn-in period, the models asymptotically sample solutions with high likelihoods and prior probabilities. The set of realizations after the burn-in period is used to estimate the posterior distribution of the model variables conditioned on the available data. At the first iteration, the model realization $\mathbf{m}_0$ is sampled from a prior distribution, whereas at the following iterations, the proposed model realization $\mathbf{m}_i$ is sampled from a proposal distribution conditioned on the model $\mathbf{m}_i$ at the previous iteration. At each iteration, the proposed realization is accepted or rejected based on the ratio of their conditional distributions conditioned on the data. Several algorithms have been presented in statistics literature with different formulations of the acceptance probability ratio and different proposal distributions. Popular MCMC methods for seismic inversion problems include the Metropolis and Metropolis-Hastings algorithms. In the Metropolis-Hastings approach, the proposed realization $\mathbf{m}'$ is drawn from a proposal distribution $g(\mathbf{m}'|\mathbf{m}_i)$ and accepted with probability p:

$$p = \min\left\{\frac{P(\mathbf{d}|\mathbf{m}')P(\mathbf{m}')g(\mathbf{m}_i|\mathbf{m}')}{P(\mathbf{d}|\mathbf{m}_i)P(\mathbf{m}_i)g(\mathbf{m}'|\mathbf{m}_i)}, 1\right\}. \tag{3}$$

In the Metropolis approach, the proposed realization $\mathbf{m}'$ is drawn from a proposal distribution where $g(\mathbf{m}'|\mathbf{m}_i) = g(\mathbf{m}_i|\mathbf{m}')$ and the acceptance probability p becomes

$$p = \min\left\{\frac{P(\mathbf{d}|\mathbf{m}')P(\mathbf{m}')}{P(\mathbf{d}|\mathbf{m}_i)P(\mathbf{m}_i)}, 1\right\}. \tag{4}$$

At each iteration, we generate a random number u from a uniform distribution in [0, 1]. If $u < p$, $\mathbf{m}'$ is accepted as a new configuration of the chain; otherwise, $\mathbf{m}'$ is rejected. It is common to assume the Gaussian PDF for the proposal distribution for its analytical formulation. The proposal distribution can also include a spatial correlation model to mimic the spatial variations of rock and fluid properties. Random realizations of the model variables can be efficiently generated using geostatistical methods to include spatial correlation models (Deutsch and Journel, 1998; Deutsch, 2002). We first formulate the MCMC approach with vertical correlation for a 1D problem by integrating vertical correlation models in the prior and proposal distribution. We then extend the approach to 2D problems by including a lateral correlation model, using two implementations based on kriging and sequential methods.

1D case

We assume a prior Gaussian distribution $\mathcal{N}(\mathbf{m};\ \boldsymbol{\mu}_m, \mathbf{\Sigma}_m)$ with locally variable prior mean $\boldsymbol{\mu}_m$ and spatially correlated prior covariance matrix $\mathbf{\Sigma}_m = \mathbf{\Sigma}_m^0 \otimes \mathbf{\Sigma}_\tau$. The likelihood function of the data $\mathbf{d}$ is Gaussian $\mathcal{N}(\mathbf{d};\ \mathbf{f}(\mathbf{m}), \mathbf{\Sigma}_\varepsilon)$ with vertically independent errors. In the MCMC, the proposal distribution is assumed to be Gaussian $\mathcal{N}(\mathbf{m}';\ \boldsymbol{\mu}_{m_i}, \alpha\mathbf{\Sigma}_m)$, where the mean $\boldsymbol{\mu}_{m_i}$ is the proposed model at the previous iteration and the covariance matrix depends on an inflation factor $\alpha < 1$. Then, the acceptance probability p in equation 4 becomes

$$p = \min\left\{\exp\left(-\frac{1}{2}(\mathcal{F}_{\text{like}}(\mathbf{m}') - \mathcal{F}_{\text{like}}(\mathbf{m}_i))\right) \times \exp\left(-\frac{1}{2}(\mathcal{F}_{\text{prior}}(\mathbf{m}') - \mathcal{F}_{\text{prior}}(\mathbf{m}_i))\right), 1\right\} \tag{5}$$

with likelihood and prior functions given by

$$\mathcal{F}_{\text{like}}(\mathbf{m}) = (\mathbf{f}(\mathbf{m}) - \mathbf{d})^T(\mathbf{\Sigma}_\varepsilon \otimes \mathbf{I}_{n_d})^{-1}(\mathbf{f}(\mathbf{m}) - \mathbf{d}), \tag{6}$$

$$\mathcal{F}_{\text{prior}}(\mathbf{m}) = (\mathbf{m} - \boldsymbol{\mu}_m)^T(\mathbf{\Sigma}_m^0 \otimes \mathbf{\Sigma}_t)^{-1}(\mathbf{m} - \boldsymbol{\mu}_m), \tag{7}$$

where $\mathbf{f}$ is the geophysical forward operator in equation 1.

The spatially dependent correlation matrix $\mathbf{\Sigma}_t$ is assumed to be a band matrix based on a prior vertical correlation function $v(t)$ of correlation length t_l and can be written as

$$\mathbf{\Sigma}_t = \begin{bmatrix} 1 & \dots & v(t_l) & \dots & \dots & \dots & 0 \\ \vdots & \ddots & \vdots & \ddots & \vdots & \vdots & \vdots \\ v(t_l) & \vdots & 1 & \vdots & v(t_l) & \vdots & \vdots \\ \vdots & \ddots & \vdots & \ddots & \vdots & \ddots & \vdots \\ \vdots & \vdots & v(t_l) & \vdots & 1 & \vdots & v(t_l) \\ \vdots & \vdots & \vdots & \ddots & \vdots & \ddots & \vdots \\ 0 & \dots & \dots & \dots & v(t_l) & \dots & 1 \end{bmatrix}. \tag{8}$$

In this formulation, we assume that the errors are uncorrelated; therefore, the covariance matrix of the data is written as $\mathbf{\Sigma}_\varepsilon \otimes \mathbf{I}_{n_d}$; however, a vertical correlation structure as in equation 8 could also be used for the data error.

In the 1D case, spatially correlated realizations can be efficiently sampled from the proposal distribution $\mathcal{N}(\mathbf{m}'; \boldsymbol{\mu}_{m_i}, \alpha\mathbf{\Sigma}_m)$ using the lower–upper (LU) decomposition method (Deutsch and Journel, 1998; Deutsch, 2002). For an accurate and efficient implementation, we calibrate parameter α to tune the variances and covariances of the proposal distribution. If local variances are too large ($\alpha > 1$), a large number of proposed models are rejected, whereas if the variances are too small ($\alpha < 1$), the algorithm might require a large number of iterations or the solution might depend on the initial model. For a detailed discussion on the mathematical definition of optimal proposal distributions, we refer the reader to Rosenthal (2011).

The approach in equations 5–8 can be extended to 2D problems, but the convergence is generally slow. Therefore, we present two approaches of a trace-by-trace inversion in which the lateral correlation is imposed in the statistical model using the previously inverted traces. The first approach is based on a sequential random path along the traces, and at each trace the prior model is computed by solving a kriging interpolation problem using the previously inverted traces as conditioning data. The second approach is based on a sequential raster (ordered) path along the traces, and at each trace the prior model is computed by imposing a similarity measure with the previously inverted adjacent trace.

2D case using kriging

For the 2D case, we propose a sequential approach in which the previously inverted traces are used as additional conditioning data. The sequential approach can be based on a random path where the traces are selected randomly or based on a raster path where the trace is visited according to their spatial ordering. We reformulate the problem in equation 2 according to a hierarchical formulation. If $\mathbf{m}^{-x}$ represents the model realizations at the previously inverted traces, then equation 2 can be rewritten as

$$\begin{aligned} P(\mathbf{m}|\mathbf{d},\mathbf{m}^{-x}) &= \frac{P(\mathbf{d},\mathbf{m}^{-x}|\mathbf{m})P(\mathbf{m})}{P(\mathbf{d},\mathbf{m}^{-x})} \\ &= \frac{P(\mathbf{d}|\mathbf{m})P(\mathbf{m}^{-x}|\mathbf{m})P(\mathbf{m})}{P(\mathbf{d})P(\mathbf{m}^{-x})} \\ &= \frac{P(\mathbf{d}|\mathbf{m})P(\mathbf{m}|\mathbf{m}^{-x})}{P(\mathbf{d})} \end{aligned} \tag{9}$$

assuming that $\mathbf{m}^{-x}$ and $\mathbf{d}$ are conditionally independent, given $\mathbf{m}$. In the first proposed approach, $\mathbf{m}^{-x}$ represents the previously inverted traces in a selected neighborhood of the current trace and the probability $P(\mathbf{m}|\mathbf{m}^{-x})$ in equation 9 is computed using kriging with a locally variable mean.

Kriging is a geostatistical method for the interpolation of spatially correlated random variables (Deutsch and Journel, 1998; Deutsch, 2002). Unlike other interpolations, kriging accounts for the spatial configuration of the measurements and the spatial correlation of the variables. The most common form of kriging is called simple kriging, where we assume that the mean of the variable of interest is known and constant in space. Given a random variable X with mean μ_X and variance σ_X^2, and a finite number of measurements $\{x_1, \ldots, x_n\}$, the interpolated value x_0^k is given by

$$x_0^k = \mu_X + \sum_{i=1}^{n} w_i(x_i - \mu_X), \tag{10}$$

where the vector of kriging weights $\mathbf{w} = [w_1, \ldots, w_n]^T$ is computed by solving a system of linear equations $\mathbf{Cw} = \mathbf{C}_0$, where the kriging matrix $\mathbf{C}$ contains the values $C(h_{i,j})$ of the spatial covariance function at the distances $h_{i,j}$ between the measurement locations, whereas the kriging vector $\mathbf{C}_0$ contains the values $C(h_{0,i})$ of the spatial covariance function at the distances $h_{0,i}$ between the measurement location and the location of interest. The prediction error can be quantified by the kriging variance:

$$\sigma_0^2 = \sigma_X^2 - \sum_{i=1}^{n} w_i C(h_{0,i}), \tag{11}$$

where σ_X^2 is the prior variance of the variable X. In the proposed method, we adopt kriging with a locally variable mean, where the mean μ_X in equation 10 is spatially variable and it is assumed to be equal to the pointwise mean of the prior distribution.

Based on equations 10 and 11, we compute the probability $P(\mathbf{m}|\mathbf{m}^{-x})$ in equation 9. The prior distribution of the model at a trace x is then a Gaussian distribution with mean $\boldsymbol{\mu}_m^k$ and covariance matrix $\boldsymbol{\Sigma}_m^k$ computed by applying kriging with a locally variable mean to the predicted model values at the previous inverted traces. The prior term $P(\mathbf{m}|\mathbf{m}^{-x})$ can then be written as

$$P(\mathbf{m}|\mathbf{m}^{-x}) = c \ \exp\left(-\frac{1}{2}((\mathbf{m}-\boldsymbol{\mu}_m^k)^T(\boldsymbol{\Sigma}_m^k)^{-1}(\mathbf{m}-\boldsymbol{\mu}_m^k))\right), \tag{12}$$

where $\mathbf{m}^{-x}$ represents the model realizations at the previous inverted traces, $\boldsymbol{\mu}_m^k$ is the kriging mean, $\boldsymbol{\Sigma}_m^k$ is a diagonal matrix with the kriging variances, and c is the normalization constant that depends on the determinant of the covariance matrix.

By including the kriging-based prior term of equation 12 in the acceptance rule of the Metropolis algorithm in equation 4, we obtain

$$\begin{aligned} p = \min\Bigg\{ &\exp\left(-\frac{1}{2}(\mathcal{F}_{\text{like}}(\mathbf{m}') - \mathcal{F}_{\text{like}}(\mathbf{m}_i))\right) \\ &\times \exp\left(-\frac{1}{2}(\mathcal{F}_{\text{krig-prior}}(\mathbf{m}') - \mathcal{F}_{\text{krig-prior}}(\mathbf{m}_i))\right), 1\Bigg\}, \end{aligned} \tag{13}$$

where

$$\mathcal{F}_{\text{krig-prior}}(\mathbf{m}) = (\mathbf{m}-\boldsymbol{\mu}_m^k)^T(\boldsymbol{\Sigma}_m^k)^{-1}(\mathbf{m}-\boldsymbol{\mu}_m^k). \tag{14}$$

In practice, we randomly select a trace according to a random path, and we apply the 1D algorithm with acceptance rule given in equation 13, which depends on the estimated models at the previous inverted traces. The kriging of the previously simulated values at the adjacent traces is selected within a moving searching neighborhood. Large moving searching neighborhoods generally lead to smooth posterior models, whereas small moving searching neighborhoods lead to a larger lateral variability.

To quantify the consistency of the kriging-based prior model and the data-informed posterior model, we compute the similarity of the two probability distributions using the Kullback-Leibler divergence:

$$\begin{aligned} D_{\text{KL}}(P(\mathbf{m}|\mathbf{d},\mathbf{m}^{-x})||P(\mathbf{m}|\mathbf{m}^{-x})) &= \int P(\mathbf{m}|\mathbf{d},\mathbf{m}^{-x}) \log\frac{P(\mathbf{m}|\mathbf{d},\mathbf{m}^{-x})}{P(\mathbf{m}|\mathbf{m}^{-x})} \mathrm{d}\mathbf{m} \\ &= \int P(\mathbf{m}|\mathbf{d},\mathbf{m}^{-x}) \log P(\mathbf{d}|\mathbf{m}) d\mathbf{m} - \log P(\mathbf{d}) \int P(\mathbf{m}|\mathbf{d},\mathbf{m}^{-x}) \mathrm{d}\mathbf{m}. \end{aligned} \tag{15}$$

The integral can be computed using the MCMC samples, by computing the mean of the negative log likelihood that is equal to the logarithm of the ratio in equation 15 apart from an additive constant. The Kullback-Leibler divergence quantifies the change of the state of information contained in the prior and in the posterior. The Kullback-Leibler divergence can reveal inconsistencies between the prior model and the likelihood, which might occur in certain geologic environments, for example, in the presence of lateral discontinuities in the data caused by a fault, or it could be caused by instability of the solution or noise in the data.

2D case using trace similarity

In the second proposed approach, we include the lateral correlation in the MCMC inversion by imposing a lateral continuity between adjacent traces in a raster path, where the traces are visited according to their spatial ordering. We adopt the same

formulation as in equation 9 with the same prior and likelihood models as the 1D case. The continuity is imposed by introducing an additional term that models the similarity between the current trace and the previous one. For a given trace x of the raster path, the spatial prior term of the model variable $\mathbf{m}$ is given by

$$P(\mathbf{m}|\mathbf{m}^{x-1}) = \exp\left(-\frac{1}{2}((\mathbf{m}-\mathbf{m}^{x-1})^T(\beta\boldsymbol{\Sigma}_m)^{-1}(\mathbf{m}-\mathbf{m}^{x-1}))\right), \tag{16}$$

where $\mathbf{m}^{x-1}$ is the mean estimate obtained from the posterior sampling of the previous trace of the path. The inflation parameter β is introduced to compute a fraction of the prior variance, and it controls the lateral correlation in the 2D model. The parameter β is tuned to reproduce the lateral correlation and guarantee a fast convergence: Values of $\beta < 1$ impose a strong lateral continuity, whereas values of $\beta > 1$ guarantee a larger variability of the proposed models. Low values lead to strongly laterally correlated models.

The Metropolis rule in equation 4 can then be rewritten as follows:

$$p = \min\left\{\begin{array}{c}\exp\left(-\frac{1}{2}(\mathcal{F}_{\text{like}}(\mathbf{m}')-\mathcal{F}_{\text{like}}(\mathbf{m}_i))\right)\times\exp\left(-\frac{1}{2}(\mathcal{F}_{\text{prior}}(\mathbf{m}')-\mathcal{F}_{\text{prior}}(\mathbf{m}_i))\right)\\ \times\exp\left(-\frac{1}{2}(\mathcal{F}_{\text{lat}}(\mathbf{m}')-\mathcal{F}_{\text{lat}}(\mathbf{m}_i))\right), 1\end{array}\right\}, \tag{17}$$

where

$$\mathcal{F}_{\text{lat}}(\mathbf{m}) = (\mathbf{m}-\mathbf{m}^{x-1})^T(\beta\boldsymbol{\Sigma}_m)^{-1}(\mathbf{m}-\mathbf{m}^{x-1}). \tag{18}$$

In this approach, at each trace we apply the 1D algorithm with the acceptance rule given in equation 18, which depends on the inverted model at the previous adjacent trace.

APPLICATION

We first illustrate the MCMC method for spatially correlated properties on a 1D seismic inversion problem; we then show the extension to a 2D problem using the two algorithms introduced in the "Methodology" section.

The first application represents a 1D inverse problem in which the input data are three synthetic seismograms. This example aims to estimate the posterior distribution of porosity and water saturation from seismic data. The vertical profile represents an oil reservoir in the Norwegian Sea. In the top part of the reservoir, the average porosity is approximately 0.25 and the oil saturation is approximately 0.80 due to the percentage of irreducible water saturation. In the lower part of the reservoir, the porosity is lower and the water saturation is close to 1. The correlation between the porosity and the water saturation is −0.6. The synthetic seismograms are computed from the well-log data using a geophysical forward operator that includes rock physics and seismic relations, namely, the stiff sand model to compute the P- and S-wave velocities and density and a seismic model to calculate the seismic response from the elastic properties. The input variables of the geophysical forward operator are porosity and water saturation, and the predicted data are the seismic amplitudes. We first apply the stiff sand model (Dvorkin et al., 2014) for a mixture of two fluids in the pore space, namely, brine and oil, and assuming a constant clay content equal to 0.2. The model assumes constant bulk and shear moduli and density for the solid phase, whereas the bulk modulus and the density of the fluid phase are computed using the Reuss average and linear average, respectively. The stiff sand model applies Hertz-Mindlin equations at the critical porosity and the modified Hashin Shtrikman upper bounds for porosity values between zero and the critical porosity to compute the dry-rock elastic moduli. Gassmann's equations are applied to compute the saturated-rock elastic properties and the corresponding P- and S-wave velocities. For this example, the critical porosity is 0.4 and the coordination number (i.e., the average number of contacts per grain) is 7. We then apply the seismic forward model using a convolutional operator. Based on the elastic properties, P- and S-wave velocities and density, calculated using the rock physics model, we compute the P-P reflection coefficients using the Aki-Richards' approximation of the Zoeppritz equations (Aki and Richards, 1980). The seismic amplitudes are finally computed as a convolution of a Ricker wavelet with a dominant frequency of 45 Hz and the P-P reflection coefficients. The seismic data include $n_d = 98$ samples and are computed with a sampling rate of 1 ms, for the angles of 15°, 30°, and 45°, assuming a signal-to-noise ratio (S/N) of five. The seismic data, with and without noise, are shown in Figure 1. We assume a truncated Gaussian distribution for porosity and water saturation. The prior mean is obtained from a low-frequency model computed by applying a filter to the actual well logs (Figure 2). We assume a prior vertical correlation model based on a Gaussian function with correlation length of 5 ms, estimated by fitting the vertical correlation function to the actual logs. The inflation parameter α is calibrated to 0.1 after a trial-and-error approach to obtain a satisfactory acceptance ratio.

We run 10^5 iterations, with a burn-in phase of approximately 1000 models. A subset of 500 realizations and the estimated posterior distribution are shown in Figure 2. The posterior mean accurately matches the actual log of porosity, but it fails to match the actual log of water saturation; however, the maximum a posteriori shows a good agreement, especially for values close to the boundary of the water saturation. Because the posterior distribution is non-Gaussian, the maximum a posteriori is numerically evaluated at each location, by approximating the posterior distribution using the histogram smoothing method and computing the argmax, i.e., the argument of the maximum.

The linear correlation coefficient between the posterior mean and the true curve is 0.90 for porosity and 0.96 for saturation, whereas the linear correlation between the maximum a posteriori and the true curve is 0.83 for porosity and 0.94 for saturation. To evaluate the uncertainty assessment, we adopt the 0.90 coverage ratio of the predictions, which defines the fraction of true values that fall within the 0.90 confidence interval. By definition, the optimal 0.90 coverage ratio is 0.90, which means that 90% of the true values fall within the 0.90 confidence interval. The 0.90 coverage ratio for porosity is 0.94, and for water saturation it is 0.70, which shows a slight underestimation of the uncertainty for water saturation, possibly due to the truncation. The convergence plot of the 10^5 iterations is shown in Figure 3. The convergence is visualized by plotting the negative logarithm of the posterior distribution, i.e., the product of the likelihood function and prior distribution apart from the normalization constants. Because the product is less than or equal to one, the logarithm is negative; therefore, we plot

the negative logarithm that has positive sign. The acceptance ratio is approximately 10%. The inversion takes approximately 150 s on a standard laptop.

We then apply the MCMC inversion methods with lateral correlation to a 2D seismic inversion problem. The seismic data are shown in Figure 4 and include three vertical sections corresponding to near, mid, and far angles. The data are computed from the synthetic reservoir model presented in Dvorkin et al. (2014), assuming an S/N equal to five. The porosity was simulated with a locally variable mean model obtained from a depth trend extracted from a real case application, and the water saturation was cosimulated from porosity assuming a linear correlation of −0.9. The 2D sections of porosity and water saturation are shown in Figure 5. The geophysical forward operator is the same as in the 1D example, and it includes the stiff sand model and the convolution of a Ricker wavelet and the P-P reflection coefficients estimated with Aki-Richards' equation. The seismic data include $n_x = 85$ traces and $n_d = 67$ samples per trace and are computed with a sampling rate of 1 ms, for the angles of 15°, 30°, and 45°. The spatial correlations functions were estimated by fitting theoretical models to the 2D sections. The prior vertical correlation is assumed to be a Gaussian function with correlation length of 5 ms, and the lateral correlation function is a spherical model with correlation length of 15 traces. The low-frequency prior model is shown in Figure 6. We apply and compare the two sequential trace-by-trace methods based on kriging and trace similarity presented in the "Methodology" section. After a trial-and-error calibration, the inflation parameter α is calibrated to 0.1 and the inflation parameter β is 1. Figure 7 shows the inverted results obtained with the kriging-based approach, whereas Figure 8 shows the inverted results obtained with the trace similarity approach. We run 10^4 iterations and compute the posterior statistics using 9000 models. Both results show accurate predictions compared with the true data set in Figure 5. The results are compared with a standard trace-by-trace MCMC approach with the same vertical correlation function but without lateral correlation model (Figure 9). The predicted models estimated using the proposed MCMC approach for spatially correlated variables show a stronger lateral continuity than the uncorrelated approach.

Figure 10 shows three randomly selected realizations obtained using preconditioning with kriging. The pointwise posterior variance maps of porosity and water saturation are shown in Figure 11, for the kriging-based approach, in which some lateral discontinuities are due to the choice of the random path used for the simulation. For a full evaluation of the posterior variance, we recommend running the MCMC algorithms multiple times with different random paths and averaging the results to avoid instability of the inversion results. The results for the trace similarity approach show similar global statistics. Figure 12 shows the 2D spatial correlation model of the posterior mean of the porosity compared to the true porosity model. The proposed method does not guarantee that the spatial correlation function is exactly reproduced. Indeed, in this case, the spatial correlation function is not exactly reconstructed, due to a slightly longer correlation length in the lateral direction. The spatial correlation model is part of the prior information that is updated according to the likelihood function of the data. In this case, the lateral continuity of the data affects the spatial correlation model of the predictions.

The linear correlation coefficient between the posterior mean and the true map is 0.88 for porosity and 0.87 for saturation, whereas the 0.90 coverage ratio for porosity is 0.86 and for water saturation is 0.68. We believe that the slight underestimation of the uncertainty is due to the spatial correlation constraints and the choice of the

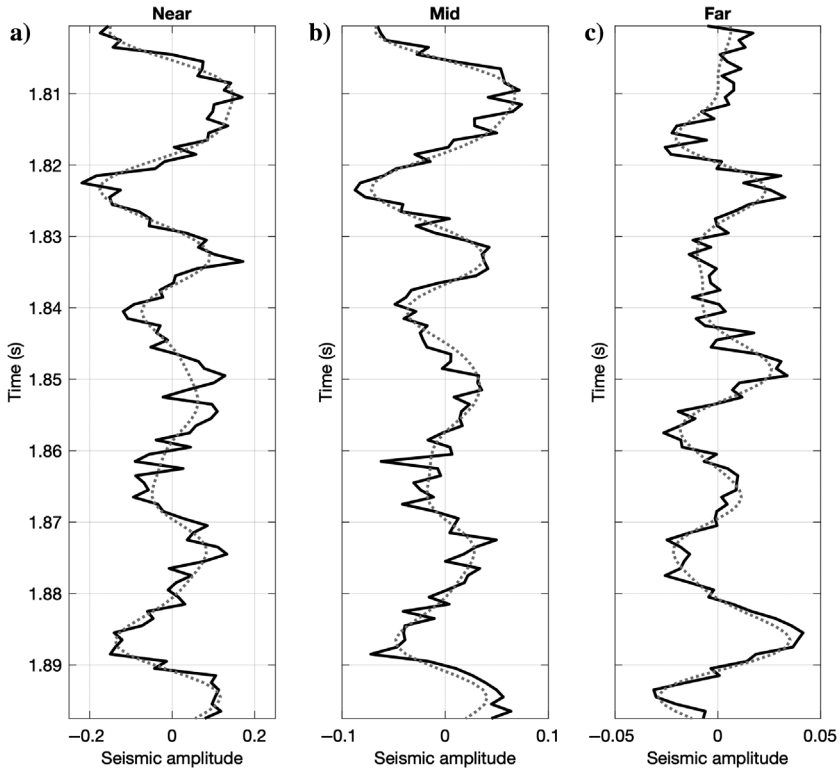

Figure 1. Synthetic seismic data set for 1D inversion: (a) near-, (b) mid-, and (c) far-angle stacks. The gray curves represent the noise-free seismic data, and the black curves represent the seismic data with noise.

random path. The calculation of the coverage ratio becomes more precise when the confidence intervals are estimated from multiple inversion runs. The convergence plots using the kriging-based and similarity-based approaches are shown in Figure 13. The preconditioned prior guarantees a faster convergence for both approaches with a burn-in phase of approximately 100 realizations. Different colors show the negative log posterior at different trace locations. The negative log posterior is defined as the negative logarithm of the product of the likelihood function and the prior distributions apart from the normalization constant. In the kriging-based approach, the first traces along the random path have a longer burn-in period, whereas the last traces in the random path have a shorter burn-in period due to the more informative prior estimated using kriging of the previously

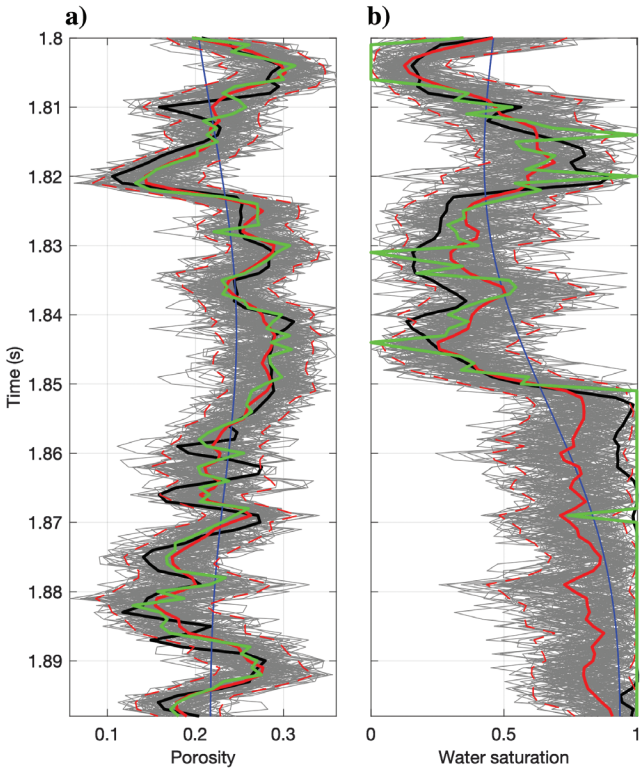

Figure 2. Inverted petrophysical properties: (a) porosity and (b) water saturation. The gray curves represent the posterior models, the green curves represent the maximum a posteriori, the red curves represent the posterior means (the dashed red curves represent the 0.90 confidence intervals), the blue curves represent the prior means, and the black curves represent the actual model.

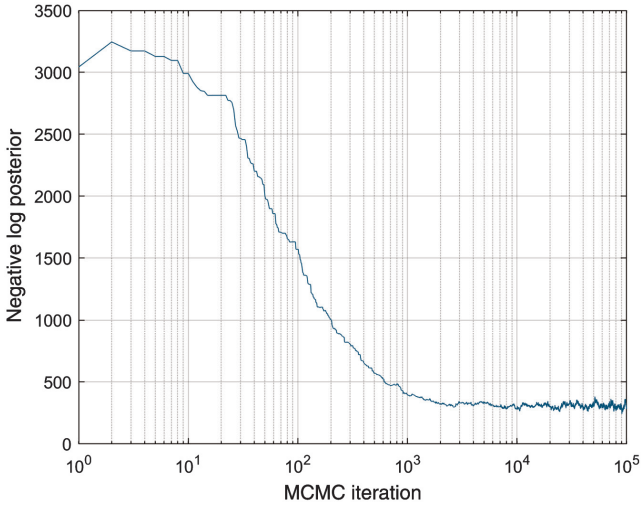

Figure 3. Convergence of the negative logarithm of the posterior distribution.

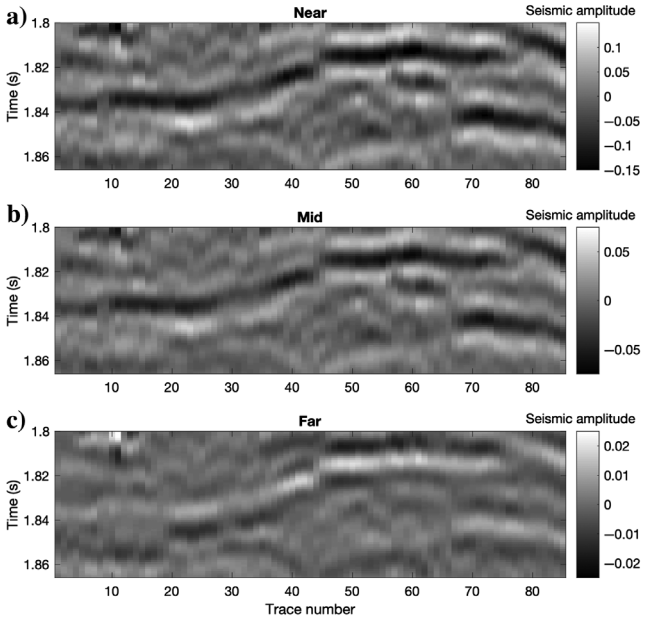

Figure 4. Synthetic seismic data set for 2D inversion: (a) near-, (b) mid-, and (c) far-angle stacks.

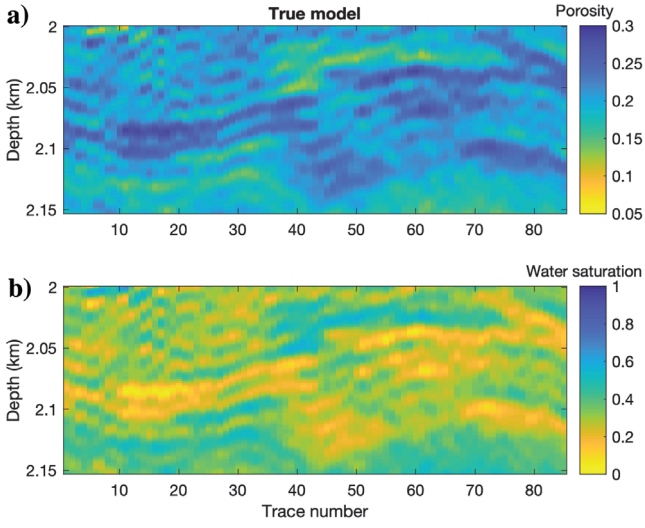

Figure 5. Actual petrophysical properties in the depth domain: (a) porosity and (b) water saturation.

inverted traces. The inversion takes approximately 18 min for 85 seismic traces on a standard laptop.

Figure 14 shows the Kullback-Leibler divergence of the posterior distribution given three different prior models: uncorrelated, kriging based, and similarity based. For the kriging- and similarity-based prior models, the Kullback-Leibler divergence is always smaller than the Kullback-Leibler divergence obtained using the laterally uncorrelated prior models. In the kriging-based approach, the Kullback-Leibler divergence decreases with the number of traces visited along the random path, due to the larger effect of the previously estimated models at adjacent locations on the kriging-based prior distribution at the current location. The trace-similarity approach shows an approximately constant Kullback-Leibler divergence, due to the proximity of the adjacent trace in the raster path compared with the kriging approach based on the random paths. Higher values of the Kullback-Leibler divergence might reveal the presence of lateral discontinuities, such as faults. Therefore, if at a given trace the Kullback-Leibler divergence of the posterior given the laterally conditioned prior is higher than the Kullback-Leibler divergence of the posterior given the laterally independent prior, the lateral constraint should not be used to reproduce the expected lateral discontinuity.

DISCUSSION

The proposed approach is computationally efficient owing to the trace-by-trace approach but still allows imposing a lateral correlation model. For 1D applications, the inversion can be efficiently applied to data sets with a large number of time samples. The extension to 2D and 3D applications with large data sets (e.g., of the

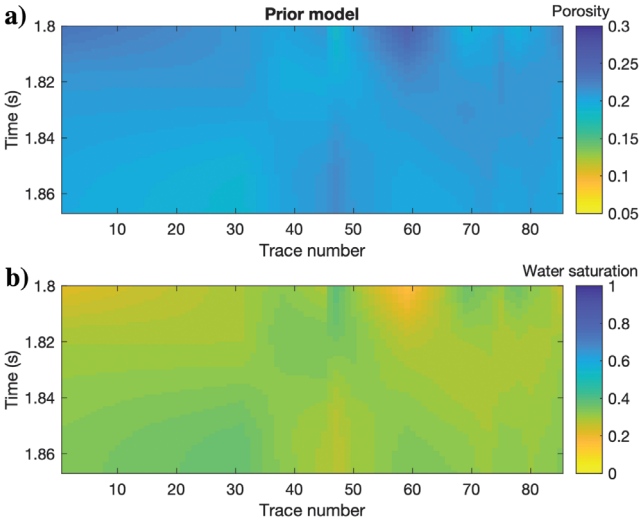

Figure 6. Prior mean of (a) porosity and (b) water saturation.

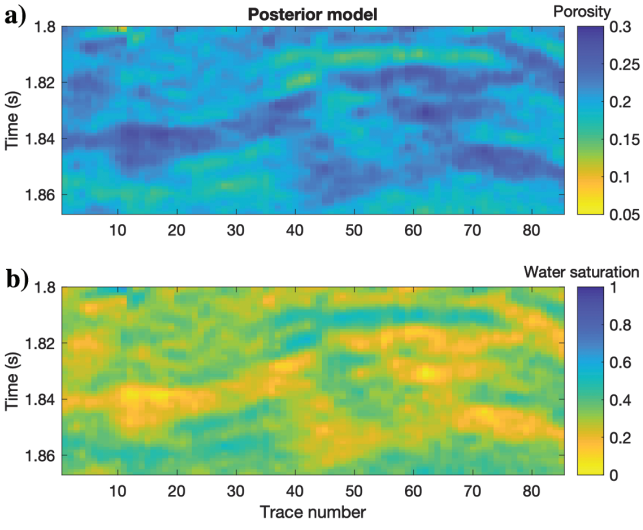

Figure 7. Posterior mean of (a) porosity and (b) water saturation obtained using preconditioning with kriging.

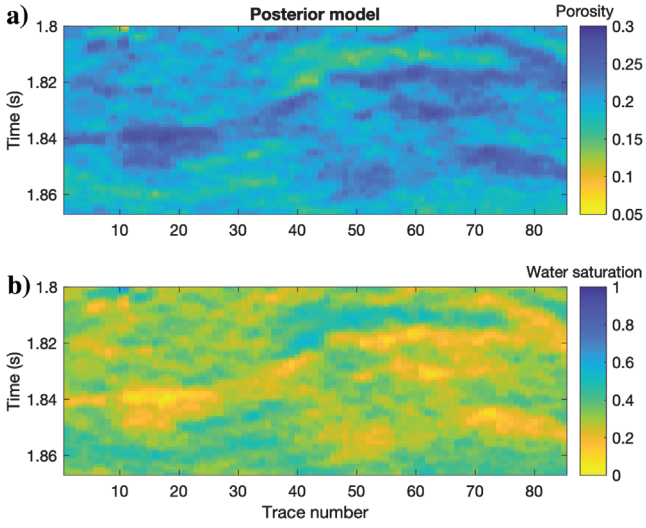

Figure 8. Posterior mean of (a) porosity and (b) water saturation obtained using preconditioning with similarity.

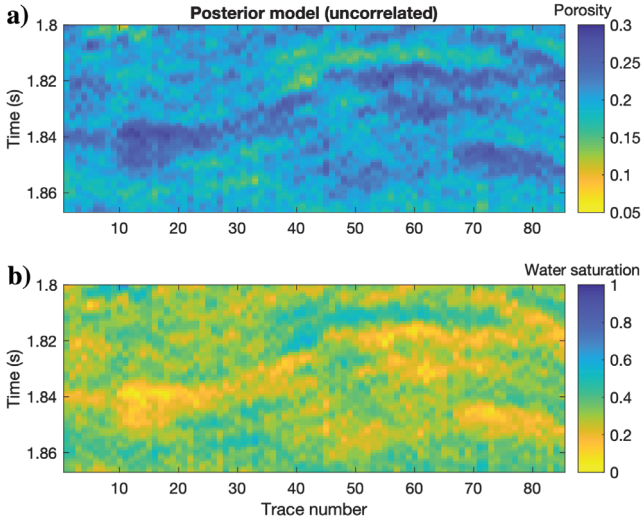

Figure 9. Posterior mean of (a) porosity and (b) water saturation obtained without prior lateral correlation.

order of 10^5 traces) might require a parallel implementation of the algorithm. The data errors are generally assumed to be spatially uncorrelated, such that the covariance matrix $\mathbf{\Sigma}_\varepsilon$ is diagonal; however, in many practical applications, the errors in the seismic data are spatially correlated due to the seismic acquisition and processing methods. If a vertical correlation model of the error is available, the 1D inversion can be applied using the full covariance matrix of the error. However, defining the parameters of the error model requires prior knowledge of seismic data acquisition and processing. The extension to 2D and 3D applications with laterally correlated errors is more challenging due to the correlation imposed by the migration operator that applies a spatial filter with correlation length associated with the Fresnel zone.

The implementation in 2D and 3D applications is based on the concept of the random path. The theoretical formulation of sequential simulations requires that all previously simulated traces should be included in the kriging interpolation. However, to reduce the computational cost, we limit the number of neighboring traces to a subset of traces that are closer to the current trace. The simulation path might also affect the local accuracy and variability of the solution. A comprehensive analysis of the effect of the simulation path on the simulated models and the definition of optimal path in terms of information loss are presented in Nussbaumer et al. (2018). In the context of stochastic inversion based on MCMC algorithms, we recommend repeating the inversion several times with different random paths to investigate the effect of the simulation path on the inversion results. The extension from 2D to 3D applications is relatively straightforward but might be limited by the computational cost of multiple runs and might require anisotropic spatial correlation functions that are challenging to calibrate with limited data.

In the proposed synthetic applications, we assume a homogeneous lithology with constant mineral volumes. The extension to petrophysical problems with variable lithologies is generally straightforward. The formulation of the proposed MCMC method is not limited by the number of model variables and can be applied to any finite number of volumetric fractions of solid and fluid phases as long as a rock-physics model can be defined and calibrated using core samples or well-log data. By introducing the volume of the main mineral component (e.g., the volume of quartz or clay in clastic reservoirs or the volume

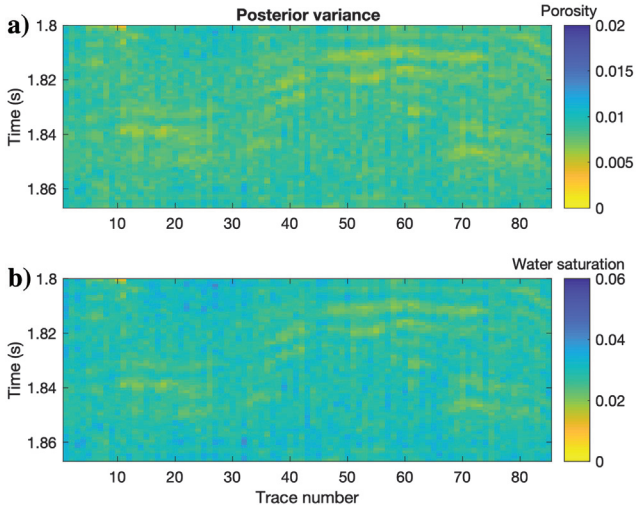

Figure 11. Posterior variance of (a) porosity and (b) water saturation obtained using preconditioning with kriging.

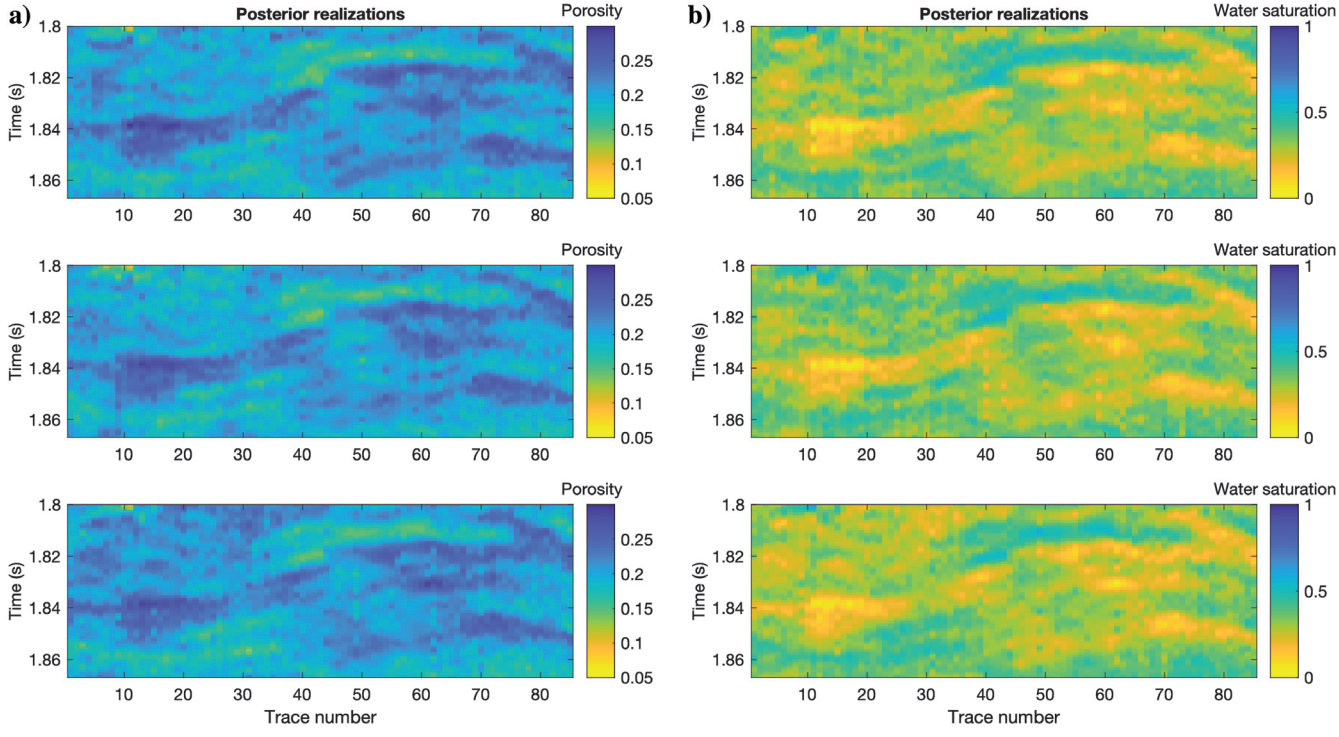

Figure 10. Three random realizations of (a) porosity and (b) water saturation obtained using preconditioning with kriging.

of calcite in carbonates), the method can be extended to multiple lithologies with the same rock-physics model (e.g., granular media models in clastic reservoirs or inclusion models in carbonates) in which the lithology variations are modeled using the effective solid elastic moduli and density computed using the Voigt and Reuss or Hashin Shtrikman mixing laws (Grana et al., 2021). If the elastic responses in multiple facies obey different rock physics relations, the MCMC can be formulated with a mixture of probability distributions (de Figueiredo et al., 2019a), in which each probability distribution corresponds to a given facies and the weights of the mixture correspond to the facies proportions. However, this algorithm requires the joint or sequential simulation of discrete (facies) and continuous (petrophysical properties) random variables and spatial correlation models for each facies. A theoretical formulation for this approach is proposed by de Figueiredo et al (2019b), but the computational cost makes it a difficult application to large data sets.

In the proposed examples, the prior distribution is assumed to be Gaussian. In general, any prior distribution can be used including Gaussian mixture models for multimodal variables (de Figueiredo et al., 2019a) or nonparametric distributions for nonsymmetric distributions (de Figueiredo et al., 2019b). For computational efficiency, it is generally possible to apply logit or normal-score transformations to perform the inversion in the transformed domain according to Gaussian assumptions (Grana et al., 2021). MCMC methods with complex prior models with spatially correlated variables have also been proposed by Hansen et al. (2012) and Zunino et al. (2015) and could be extended to the proposed approach for continuous properties.

One of the critical aspects of the application of this methodology to real case studies is the calibration of the hyperparameters of the prior and forward models. The rock-physics model might require laboratory experiments of the rock and fluid parameters (e.g., the bulk and shear moduli and density of the mineral and fluid components) and well-log calibration to fit empirical constants (e.g., the average coordination number or aspect ratio). Similarly, spatial correlation models must be calibrated using available data and nearby field information: The vertical correlation function can generally be defined at the well location by fitting theoretical models to the experimental function, whereas lateral correlation is often assumed a priori based on nearby fields or prior geologic knowledge of the area. Theoretically, it is possible to calibrate the lateral correlation function from seismic data; however, one of the main challenges of this approach is the potential bias in the lateral continuity of the processed seismic data due to the migration operator in the Fresnel zone.

The Kullback-Leibler divergence is used to illustrate the advantages of the spatially correlated approach compared to the uncorrelated one and to identify local discontinuities that might be due to instability of the solution, noise in the data, or local discontinuities. Other metrics could be used, including the Wasserstein distance or the Kantorovich-Rubinstein metric and the Jensen-Shannon divergence. The Wasserstein distance is a distance function defined

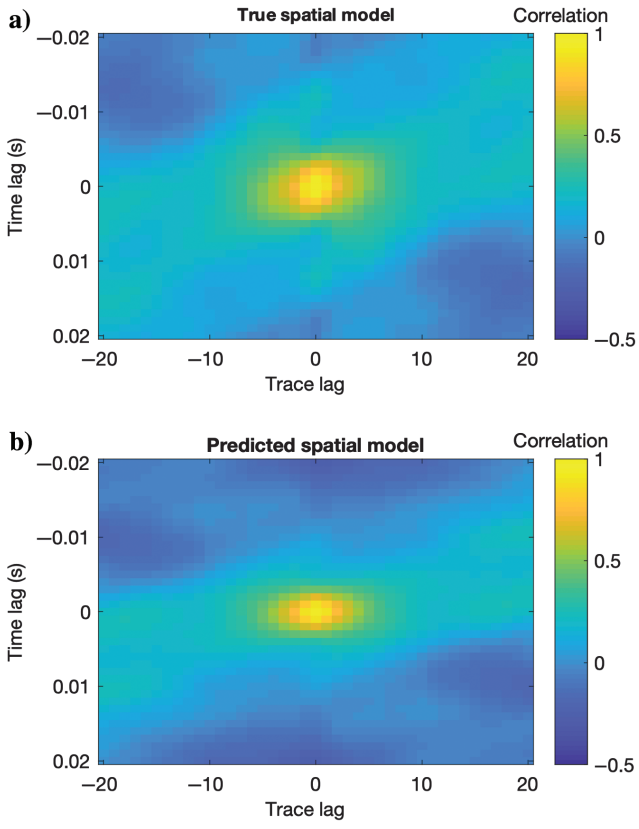

Figure 12. Posterior spatial correlation model of porosity obtained using (a) preconditioning with kriging compared to (b) the model estimated from true data.

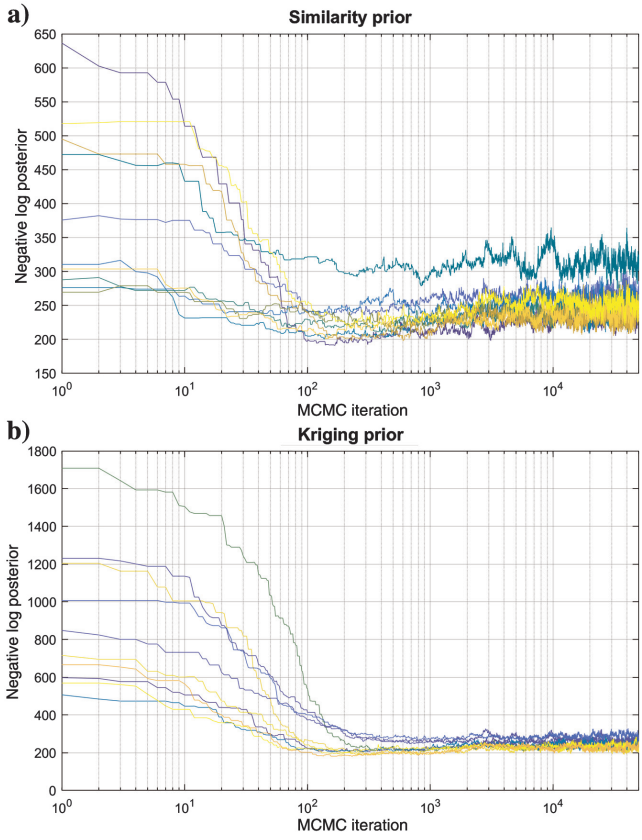

Figure 13. Convergence plot of the negative logarithm of the posterior distribution for multiple traces: the (a) similarity-based approach and (b) kriging-based approach.

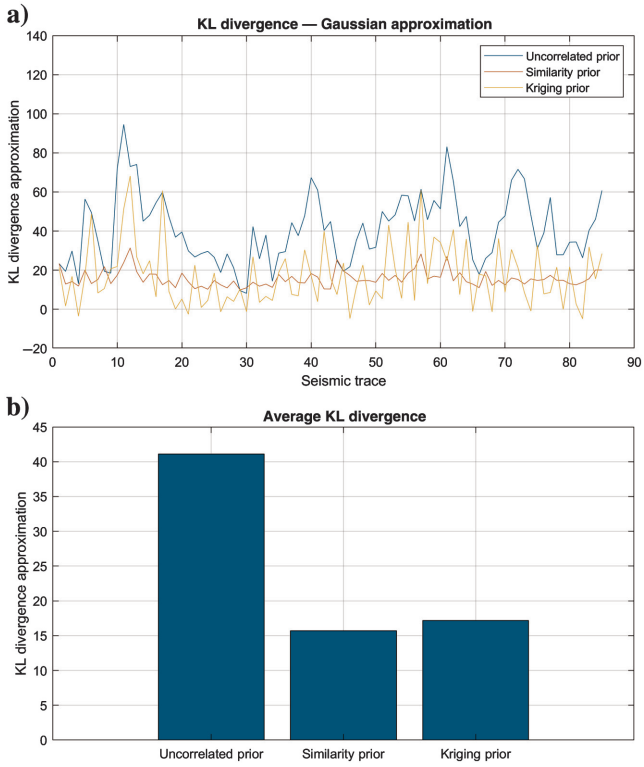

Figure 14. Kullback-Leibler divergence of the posterior distribution given the prior distribution: (a) a comparison of the Kullback-Leibler divergence for the different prior models at each trace and (b) the average Kullback-Leibler divergence for the different prior models.

between probability distributions on a given metric space, but it is less analytically tractable than the Kullback-Leibler divergence. The Jensen-Shannon divergence is defined based on the Kullback-Leibler divergence, but it is symmetric by definition. We adopt the Kullback-Leibler divergence due to its direct connection to information theory because it quantifies the change of the state of information from one distribution to the other.

CONCLUSION

We presented an MCMC method for the seismic inversion problem to estimate the posterior distribution of petrophysical properties. The method is specifically developed for vertically correlated random variables by introducing a vertical covariance model in the prior distribution. The extension to multidimensional problems is based on a sequential trace-by-trace approach in a hierarchical Bayesian formulation, in which the prior model combines the prior distribution of the model variables and a lateral correlation model. We presented two efficient approaches: The first approach is based on a kriging approach with a locally variable mean, whereas the second approach is based on a similarity measure of adjacent traces. Both approaches are computationally efficient and can be implemented on standard laptops. The applications demonstrate that the proposed method accurately predicts the model variables, quantifies the model uncertainty, and reproduces the expected spatial correlation in the vertical and lateral directions.

ACKNOWLEDGMENT

The authors acknowledge the School of Energy Resources at the University of Wyoming, the Nielson Energy Fellowship, LTrace, and BP (sponsor of the Bayesian Learning Consortium).

DATA AND MATERIALS AVAILABILITY

Data associated with this research are available and can be obtained by contacting the corresponding author.

REFERENCES

Aki, K., and P. G. Richards, 1980, Quantitative seismology: Theory and methods: Freeman.
Aleardi, M., and A. Salusti, 2020a, Markov chain Monte Carlo algorithms for target-oriented and interval-oriented amplitude versus angle inversions with non-parametric priors and non-linear forward modellings: Geophysical Prospecting, **68**, 735–760, doi: 10.1111/1365-2478.12876.
Aleardi, M., and A. Salusti, 2020b, Hamiltonian Monte Carlo algorithms for target- and interval-oriented amplitude versus angle inversions: Geophysics, **85**, no. 3, R177–R194, doi: 10.1190/geo2019-0517.1.
Avseth, P., T. Mukerji, and G. Mavko, 2010, Quantitative seismic interpretation: Applying rock physics tools to reduce interpretation risk: Cambridge University Press.
Azevedo, L., D. Grana, and L. de Figueiredo, 2020, Stochastic perturbation optimization for discrete-continuous inverse problems: Geophysics, **85**, no. 5, M73–M83, doi: 10.1190/geo2019-0520.1.
Azevedo, L., R. Nunes, A. Soares, E. C. Mundin, and G. S. Neto, 2015, Integration of well data into geostatistical seismic amplitude variation with angle inversion for facies estimation: Geophysics, **80**, no. 6, M113–M128, doi: 10.1190/geo2015-0104.1.
Azevedo, L., and A. Soares, 2017, Geostatistical methods for reservoir geophysics: Springer.
Babasafari, A., S. Rezaei, A. Salim, S. Kazemeini, and D. Ghosh, 2021, Petrophysical seismic inversion based on lithofacies classification to enhance reservoir properties estimation: A machine learning approach: Journal of Petroleum Exploration and Production, **11**, 673–684, doi: 10.1007/s13202-020-01013-0.
Bortoli, L. J., F. Alabert, A. Haas, and A. Journel, 1993, Constraining stochastic images to seismic data, *in* A. O. Soares, ed., Geostatistics Tróia '92: Quantitative Geology and Geostatistics, 5, 325–337: Springer.
Bosch, M., T. Mukerji, and E. F. González, 2010, Seismic inversion for reservoir properties combining statistical rock physics and geostatistics: A review: Geophysics, **75**, no. 5, 75A165–75A176, doi: 10.1190/1.3478209.
Buland, A., O. Kolbjørnsen, R. Hauge, Ø. Skjæveland, and K. Duffaut, 2008, Bayesian lithology and fluid prediction from seismic prestack data: Geophysics, **73**, no. 3, C13–C21, doi: 10.1190/1.2842150.
Buland, A., and H. Omre, 2003, Bayesian linearized AVO inversion: Geophysics, **68**, 185–198, doi: 10.1190/1.1543206.
Connolly, P. A., and M. J. Hughes, 2016, Stochastic inversion by matching to large numbers of pseudo-wells: Geophysics, **81**, no. 2, M7–M22, doi: 10.1190/geo2015-0348.1.
Cyz, M., and L. Azevedo, 2020, Direct geostatistical seismic amplitude versus angle inversion for shale rock properties: IEEE Transactions on Geoscience and Remote Sensing, **59**, 5335–5344, doi: 10.1109/TGRS.2020.3017091.
de Figueiredo, L. P., D. Grana, M. Roisenberg, and B. B. Rodrigues, 2019a, Gaussian mixture Markov chain Monte Carlo method for linear seismic inversion: Geophysics, **84**, no. 3, R463–R476, doi: 10.1190/geo2018-0529.1.
de Figueiredo, L. P., D. Grana, M. Roisenberg, and B. B. Rodrigues, 2019b, Multimodal Markov chain Monte Carlo method for nonlinear petrophysical seismic inversion: Geophysics, **84**, no. 5, M1–M13, doi: 10.1190/geo2018-0839.1.
Deutsch, C. V., 2002, Geostatistical reservoir modelling: Oxford University Press.
Deutsch, C. V., and A. G. Journel, 1998, GSLIB: Geostatistical software library and user's guide: Oxford University Press.
Doyen, P. M., 1988, Porosity from seismic data: A geostatistical approach: Geophysics, **53**, no. 10, 1263–1275.
Doyen, P., 2007, Seismic reservoir characterization: EAGE.
Dvorkin, J., M. Gutierrez, and D. Grana, 2014, Seismic reflections of rock properties: Cambridge University Press.
Eidsvik, J., P. Avseth, H. Omre, T. Mukerji, and G. Mavko, 2004, Stochastic reservoir characterization using prestack seismic data: Geophysics, **69**, 978–993, doi: 10.1190/1.1778241.

González, E. F., T. Mukerji, and G. Mavko, 2008, Seismic inversion combining rock physics and multiple-point geostatistics: Geophysics, **73**, no. 1, R11–R21, doi: 10.1190/1.2803748.
Grana, D., 2016, Bayesian linearized rock-physics inversion: Geophysics, **81**, no. 6, D625–D641, doi: 10.1190/geo2016-0161.1.
Grana, D., and E. Della Rossa, 2010, Probabilistic petrophysical-properties estimation integrating statistical rock physics with seismic inversion: Geophysics, **75**, no. 3, O21–O37, doi: 10.1190/1.3386676.
Grana, D., T. Mukerji, and P. Doyen, 2021, Seismic reservoir modeling: Theory, examples, and algorithms: John Wiley & Sons.
Grana, D., T. Fjeldstad, and H. Omre, 2017, Bayesian Gaussian mixture linear inversion for geophysical inverse problems: Mathematical Geosciences, **49**, 1–23, doi: 10.1007/s11004-016-9671-9.
Grana, D., T. Mukerji, J. Dvorkin, and G. Mavko, 2012, Stochastic inversion of facies from seismic data based on sequential simulations and probability perturbation method: Geophysics, **77**, no. 4, M53–M72, doi: 10.1190/geo2011-0417.1.
Haas, A., and O. Dubrule, 1994, Geostatistical inversion — A sequential method of stochastic reservoir modelling constrained by seismic data: First Break, **12**, 561–569, doi: 10.3997/1365-2397.1994034.
Hansen, T. M., K. S. Cordua, B. H. Jacobsen, and K. Mosegaard, 2014, Accounting for imperfect forward modeling in geophysical inverse problems — Exemplified for crosshole tomography: Geophysics, **79**, no. 3, H1–H21, doi: 10.1190/geo2013-0215.1.
Hansen, T. M., K. S. Cordua, and K. Mosegaard, 2012, Inverse problems with non-trivial priors: Efficient solution through sequential Gibbs sampling: Computational Geosciences, **16**, 593–611, doi: 10.1007/s10596-011-9271-1.
Hansen, T. M., A. G. Journel, A. Tarantola, and K. Mosegaard, 2006, Linear inverse Gaussian theory and geostatistics: Geophysics, **71**, no. 6, R101–R111, doi: 10.1190/1.2345195.
Jeong, C., T. Mukerji, and G. Mariethoz, 2017, A fast approximation for seismic inverse modeling: Adaptive spatial resampling: Mathematical Geosciences, **49**, 845–869, doi: 10.1007/s11004-017-9693-y.
Jullum, M., and O. Kolbjørnsen, 2016, A Gaussian based framework for Bayesian inversion of geophysical data to rock properties: Geophysics, **81**, no. 3, R75–R87, doi: 10.1190/geo2015-0314.1.
Larsen, A. L., M. Ulvmoen, H. Omre, and A. Buland, 2006, Bayesian lithology/fluid prediction and simulation on the basis of a Markov-chain prior model: Geophysics, **71**, no. 5, R69–R78, doi: 10.1190/1.2245469.
Mavko, G., T. Mukerji, and J. Dvorkin, 2020, The rock physics handbook: Cambridge University Press.
Mosegaard, K., and A. Tarantola, 1995, Monte Carlo sampling of solutions to inverse problems: Journal of Geophysical Research, **100**, 12431–12447, doi: 10.1029/94JB03097.
Mukerji, T., A. Jørstad, P. Avseth, G. Mavko, and J. R. Granli, 2001, Mapping lithofacies and pore-fluid probabilities in a North Sea reservoir: Seismic inversions and statistical rock physics: Geophysics, **66**, 988–1001, doi: 10.1190/1.1487078.
Nussbaumer, R., G. Mariethoz, E. Gloaguen, and K. Holliger, 2018, Which path to choose in sequential Gaussian simulation: Mathematical Geosciences, **50**, 97–120, doi: 10.1007/s11004-017-9699-5.
Priezzhev, I., P. Veeken, S. Egorov, and U. Strecker, 2019, Direct prediction of petrophysical and petroelastic reservoir properties from seismic and well-log data using nonlinear machine learning algorithms: The Leading Edge, **38**, 949–958, doi: 10.1190/tle38120949.1.
Rimstad, K., P. Avseth, and H. Omre, 2012, Hierarchical Bayesian lithology/fluid prediction: A North Sea case study: Geophysics, **77**, no. 2, B69–B85, doi: 10.1190/geo2011-0202.1.
Rosenthal, J. S., 2011, Optimal proposal distributions and adaptive MCMC, *in* S. Brooks, A. Gelman, G. Jones, and X. L. Meng, eds., Handbook of Markov chain Monte Carlo: CRC Press, 93–112.
Sambridge, M., and K. Mosegaard, 2002, Monte Carlo methods in geophysical inverse problems, *in* S. Brooks, A. Gelman, G. Jones, and X. L. Meng, eds., Reviews of Geophysics: CRC press, 93–112, doi: 10.1029/2000RG000089.
Scales, J. A., and L. Tenorio, 2001, Prior information and uncertainty in inverse problems: Geophysics, **66**, 389–397, doi: 10.1190/1.1444930.
Sen, M., and P. Stoffa, 1996, Bayesian inference, Gibbs sampler and uncertainty estimation in geophysical inversion: Geophysical Prospecting, **44**, 313–350, doi: 10.1111/j.1365-2478.1996.tb00152.x.
Soares, A., J. D. Diet, and L. Guerreiro, 2007, Stochastic inversion with a global perturbation method: EAGE Conference on Petroleum Geostatistics, cp-32, doi: 10.3997/2214-4609.201403048.
Tarantola, A., 2005, Inverse problem theory: SIAM.
Tarantola, A., and B. Valette, 1982, Inverse problems = quest for information: Journal of Geophysics, **50**, 159–170.
Ulrych, T. J., M. D. Sacchi, and A. Woodbury, 2001, A Bayes tour of inversion: A tutorial: Geophysics, **66**, 55–69, doi: 10.1190/1.1444923.
Ulvmoen, M., and H. Omre, 2010, Improved resolution in Bayesian lithology/fluid inversion from prestack seismic data and well observations — Part 1: Methodology: Geophysics, **75**, no. 2, R21–R35, doi: 10.1190/1.3294570.
Zunino, A., K. Mosegaard, K. Lange, Y. Melnikova, and T. Hansen, 2015, Monte Carlo reservoir analysis combining seismic reflection data and informed priors: Geophysics, **80**, no. 1, R31–R41, doi: 10.1190/geo2014-0052.1.

Biographies and photographs of the authors are not available.